Journal of Electroceramics, 9, 125–135, 2002

Microstructure and Properties of Solution Deposited, Nb-Doped PZT Thin Films

M. ES-SOUNI,* A. PIORRA, C.-H. SOLTERBECK, S. IAKOVLEV & M. ABED
University of Applied Sciences, Institute of Materials and Surface Technology (IMST), Kiel, Germany

Submitted April 3, 2002; Revised September 30, 2002; Accepted October 17, 2002

Abstract. Nb doped PZT films with Nb concentrations of 0, 5, 8 and 12 mol% are being processed via chemical solution deposition on platinized Silicon substrates. An original processing route including seed layer and additional PbO coating is presented whereby homogeneous, pyrochlore free microstructures with 111/100 texture are obtained. The temperature dependence of the dielectric constant shows diffuse peaks corresponding to the paraelectric to ferroelectric transition. The transition temperature is found to decrease from 325°C to 220°C with increasing Nb content. Nb is however found to lead to a substantial increase in the dielectric constant in comparison to non-doped PZT. The dependence of the dielectric constant on DC bias field is also reported. Strong asymmetries towards positive values both in the values of the dielectric constant and coercive fields are obtained at room temperature, and become replenished at 100°C. This is interpreted in terms of space charge effects on the pinning of domain walls. Furthermore, the loss tangent shows a relaxation peak which shifts to higher frequencies with increasing Nb content, and suggests that Nb-doping affects the dielectric properties of the interfacial layer. Finally, Nb addition is found to lead to slant hysteresis loops with lower remnant polarization and coercive field.

Keywords: PZT, Nb-doping, solution deposition, seed layer, electrical properties

1. Introduction

Ferroelectric ceramic thin films based on the oxides $Pb(Zr_x\ Ti_{1-x})O_3$ (PZT) with a perovskite-like structure have been shown to be of major technological interest for many sensor and actuating applications due to their piezoelectric, electro-optic and pyroelectric properties [1–3]. Furthermore, the suitable ferroelectric properties and the relatively high dielectric permittivity, particularly for compositions near the morphotropic phase boundary ($Pb(Zr_{0.52}, Ti_{0.48})O_3$) make PZT a promising material for thin film based capacitors in ferroelectric DRAMS [3, 4]. Many processing routes for thin film PZT, including laser ablation, Sputter techniques, CVD and chemical solution deposition (CSD) methods have been reported [5]. Nevertheless, it is well accepted that CSD constitutes the method of choice for low-cost processing of PZT thin films with controlled stoichiometry and microstructure [6]; additional advantages lie in the relatively low processing temperatures, the quite simple and cost effective preparation methods, as well as versatile laboratory equipment.

The properties of PZT are known to be affected by microstructure and the nature and amount of doping elements. Both doping on A (Pb) and B (Zr, Ti) sites with isovalent and/or aliovalent elements can affect the microstructure development and electrical properties of the thin films. Particularly donor elements like La on Pb or Nb on (Zr, Ti) sites have been reported to positively influence the long term reliability of PZT thin films [7–12], although the dielectric/ferroelectric properties seem to be rather decreased in contrast to what should be expected from effects on bulk ceramics [10–12]. In this respect, the microstructure and ferroelectric properties of Nb doped PZT (PNZT) thin films with Nb concentrations in the range from 0 to 0.05 mol were investigated by Klissurska et al. [11, 12]. They concluded that Nb additions higher than 0.02 were harmful

*To whom all correspondence should be addressed.

to ferroelectric properties because of the occurrence of surface pyrochlore [11] and the existence of pinning centres [12].

In a recent work [13] we reported the effects of Nb doping on the crystallisation kinetics of CSD PZT thin films on Pt bottom electrodes. It has been shown that 5 mol% Nb on B sites lead to a slower crystallization kinetics than non doped PZT. Furthermore, microstructure control was found difficult to achieve, and the occurrence of surface pyrochlore was found to lead to poor ferroelectric properties in comparison to non-doped PZT.

The aim of the present work is to investigate the possibilities of microstructure control in PNZT thin films containing up to 12 mol% Nb and to investigate in more details the effects of Nb on the electrical properties of PNZT thin films, including impedance measurements, and their dependence on temperature.

2. Experimental

The starting reagents for the precursor solution were $Pb(CH_3COO)_2 \cdot 3H_2O$, Zr-n-propoxide, Ti-isopropoxide and Nb-5-n-butoxide which were mixed to give the required stoichiometry. The stock solution was stabilized with 1 mol Acetylancetone and diluted with 2-metoxyethanol to give a concentration of 0.6 mol. Figure 1 shows a flow diagram for the sol preparation and the stoichiometries used.

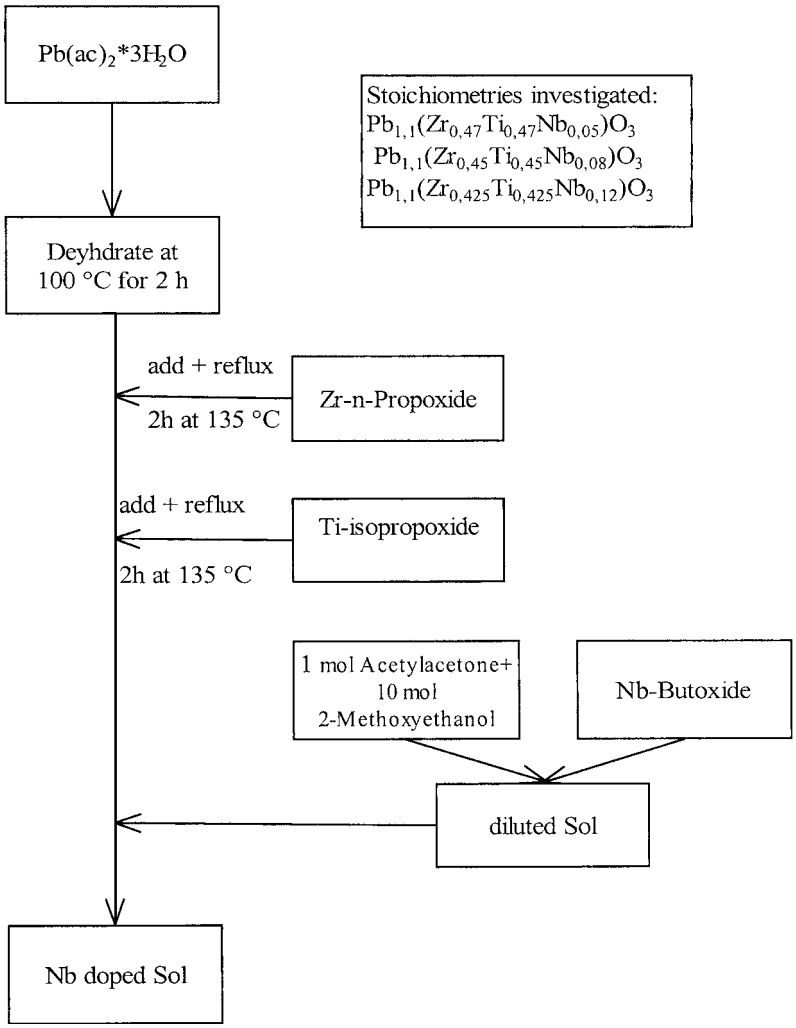

Fig. 1. Flow diagram for precursor solution preparation.

Spin coating was achieved on pre-annealed (700°C for 30 min) (111)- Pt (100 nm)/TiO_2 (10 nm)/SiO_2/Si substrates. A first set of specimens were processed according to the following sequences: pyrolysis of the first layer on a hot plate at 350°C for 30 min before a second coating was performed. After renewed pyrolysis the coated substrates were pre-annealed for 15 min at 500°C. For all specimens, 3 coating sequences were performed. The final annealing was conducted at 700°C for 30 minutes. A second set of specimens included a crystallized first layer at 700°C for 30 minutes to act as a seed layer. All other coating sequences and pyrolysis conditions remained unchanged. Before final annealing a PbO layer was coated on the third layer in order to compensate for lead evaporation during high temperature annealing. For comparison a PZT (0.0 Nb) thin film was also prepared using the same procedure, with however a shorter annealing time of 10 minutes at 700°C. The final thickness determined by a precision ellipsometer and controlled on cross section SEM specimens was in the range of 300 to 350 nm for all specimens. Microstructure and phase composition were studied by scanning electron microscopy (SEM) and X-ray diffractometry (XRD). Preliminary investigations of the chemistry of the seed layer of PZT were performed by means of X-ray photoelectron spectroscopy (XPS) and depth profiling. For electrical measurements, capacitors were obtained by sputtering Platinum top electrodes of 0.6 mm diameter through a shadow mask. Post top electrode deposition annealing at 400°C for 10 min was performed. The ferroelectric properties were measured using an RT6000S ferroelectric test system (Radiant technologies) with 2 ms square pulses and voltage amplitudes up to 19 V.

The RT6000S is a virtual ground measuring system. It measures the current flow through the sample in response to the applied drive voltage. For hysteresis measurements the drive profile consists of a stepped traingular signal. For polarization measurements short triangular pulses are applied, of which the first one sets the sample into a defined state and the following ones sense several kind of polarization. Compared to the standard Sawyer tower the sense capacitor is replaced with a measurement circuit, which keeps the sample low at a virtual ground potential and integrates the flowing charge. The advantages of this system are the lack of the back voltage of the Sawyer tower and a reduced influence of parasitic capacitances. Temperature and frequency dependences of the dielectric properties were studied by a computer controlled Agilent 4192A impedance analyser using an AC drive amplitude of 50 mV_{p-p}.

3. Experimental Results

3.1. Microstructures

The XRD diagrams shown in Fig. 2 reveal that the thin films are fully crystallized in the perovskite phase.

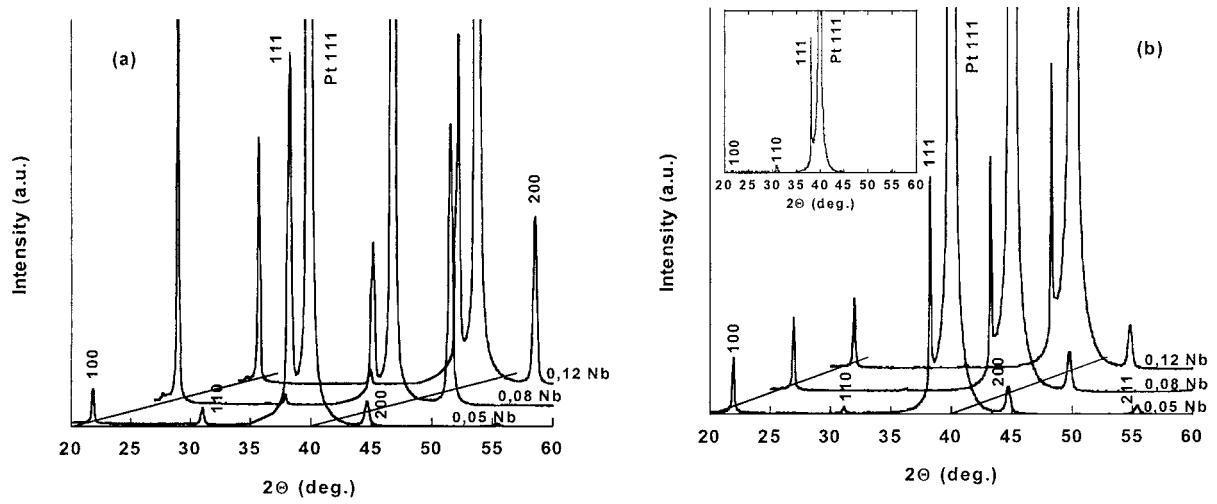

Fig. 2. XRD diagrams of the PNZT thin films: (a) without seed layer; (b) with seed layer and additional PbO coating. The inset in (b) shows the XRD diagram of PZT (0% Nb).

Table 1. Peak intensity ratios of the investigated thin films.

	Without seed layer		With seed layer and PbO	
	α_{111}	α_{100}	α_{111}	α_{100}
0.0 Nb[a]	0.01 [14]	0.94 [14]	0.93	0.015
0.05 Nb	0.87	0.089	0.78	0.19
0.08 Nb	0.28	0.69	0.74	0.23
0.12 Nb	0.57	0.40	0.76	0.19

[a]PZT powder: $\alpha_{111} = 0.09$; $\alpha_{100} = 0.07$.

However, depending on whether a seed layer is present or not, the formation of specific film textures can be noticed. The film preferential orientation, α_{hkl}, can be qualitatively calculated using [14]:

$$\alpha_{hkl} = I_{hkl} / \Sigma I_{hkl}, \tag{1}$$

where I_{hkl} is the intensity of the corresponding lattice reflection. Table 1 shows the results obtained-for α_{111} and α_{100}. The films crystallized without seed layer show a quite complex picture consisting of (100) preferred texture for PZT (not shown [15]), (111) texture for the film with 0.05 mol Nb, then a (100)/(111) with predominance of (100) for the one containing 0.08 Nb and finally a (111)/(100) texture for the film with 0.12 Nb. In contrast, the films crystallized with a seed layer all show a high degree of microstructure control with in all Nb containing films a (111)/100 texture and similar α_{111} and α_{100} values.

In order to gain more insight into the chemistry of the first deposited thin film layer (seed layer), XPS depth profiles were taken on a single PZT layer deposited on Pt and annealed at 700°C. Figure 3 shows

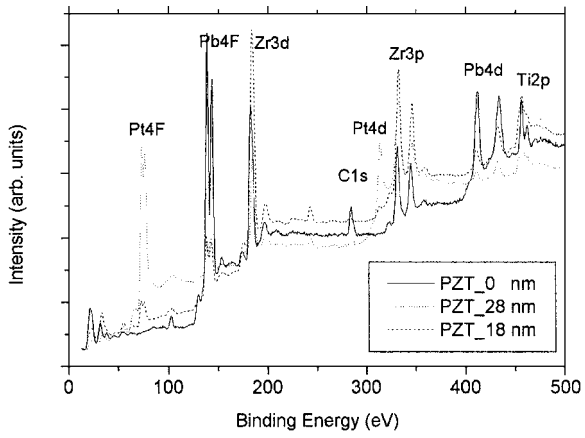

Fig. 3. XPS depth profiling analysis of the seed layer.

preliminary results where the XPS spectra before and after depth profiling are displayed. Comparison of the spectra indicates that before sputtering Pb, Zr and Ti are present at the surface, with a relatively high signal intensity for Pb. After 18 nm depth profiling, Pt appears, accompanied by a drastic decrease of the Pb and an increase in Zr signal intensities. Further sputtering leads to a strong increase in the Pt intensity while Zr and Ti decrease; the intensity of Pb continues to decrease, though more slowly. These results suggest a compositional gradient in the thin film layer with a surface enrichment in PbO. The presence of Pt at low depths beneath the surface can be explained either by the formation of an interfacial reaction layer between Zr and Pt, or in terms of the roughness of the Pt layer being high in comparison to the thickness of the PZT thin film, so that depth profiling would uncover the hillocks of the Pt layer. In both cases, a disturbed first layer is obtained with a chemistry different from that of the bulk film. However, more work is needed to elucidate the chemistry and structure of the first deposited layer. Using the results above, we can estimate the thickness of the seed layer to be in the range of 20 nm.

SEM investigations reveal different surface morphologies of both sets of specimens. The films crystallized without seed layer consist of a heterogeneous microstructure with a fine grained matrix and coarse globular grains, Fig. 4(a)–(c) (the surface morphology of PZT consists of rosette-like structure with lead deficient regions (LDR) [15]). Dark contrast areas, particularly for higher Nb concentrations, which indicate the presence of LDR, can also be seen.

For the second set of specimens with seed layer and additional PbO coating, the microstructures obtained are illustrated in Fig. 5(a)–(d). As can be seen a homogeneous, fine grained microstructure is obtained for all specimens. A relatively fine microstructure is obtained for the thin films with 0 and 0.05 Nb, and the absence of LDR can also be noticed. The existence of scattered coarser grains in these films can be attributed to grain growth due to high crystallization kinetics at 700°C. As the Nb content increases, a larger grain size is obtained. The reproducibility of the microstructures was checked on several samples using the same processing conditions. At the present stage it is not possible to explain the coarsening of microstructure or change in the grain morphology with increasing Nb content. Because crystallization of perovskite takes place from pyrochlore, the morphological change of the perovskite

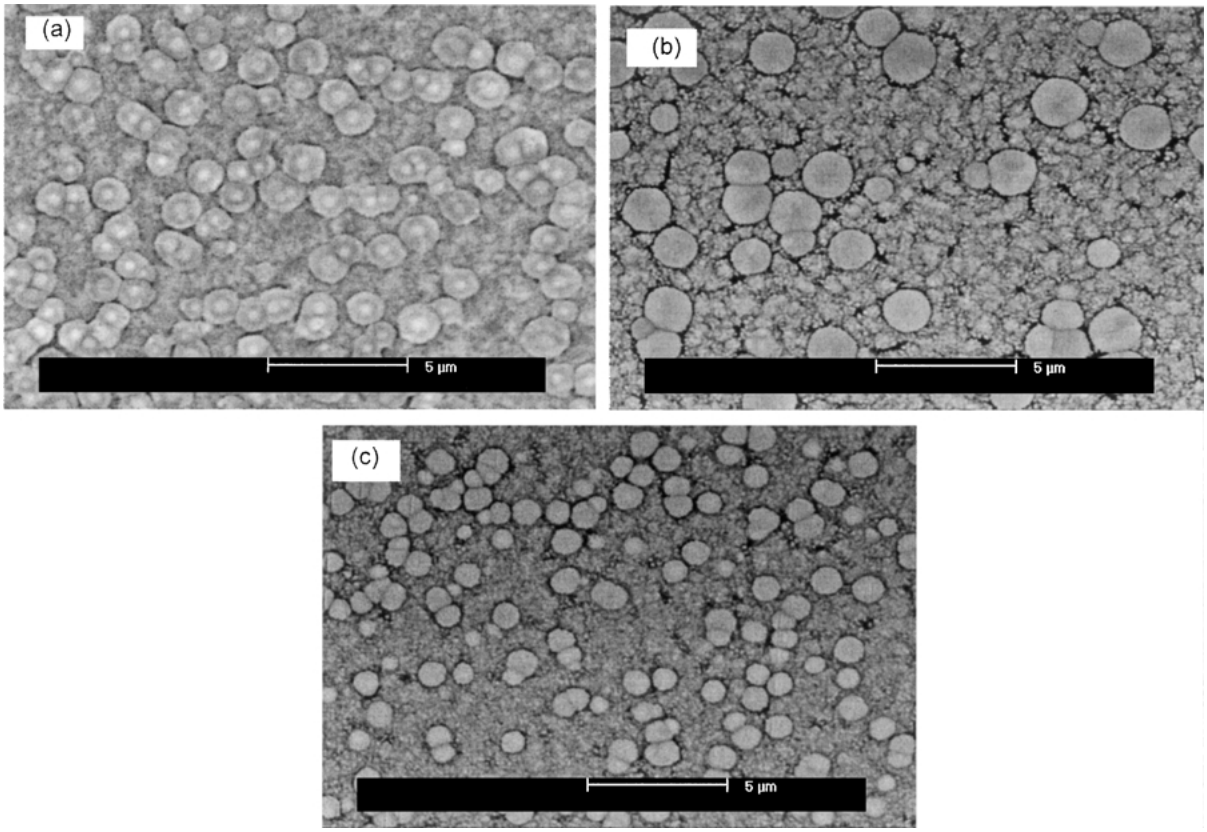

Fig. 4. Microstructures of the PNZT thin films crystallized without a seed layer: (a) 0.05, (b) 0.08 and (c) 0.12 mol Nb.

phase might have its origins in some morphological changes of pyrochlore caused by increasing Nb content.

3.2. *Electrical Properties*

3.2.1. Temperature dependence of the dielectric constant. The electrical properties were determined for the thin films processed with seed layers and PbO coatings. The temperature dependence of the dielectric constant is shown in Fig. 6 (for the Nb containing films). For all thin film compositions, the small signal dielectric constant increases with increasing temperature. A shoulder is obtained at around 100°C, and can be attributed to mobile domain walls [16]. At higher temperatures diffuse maxima the loci of which depend on the Nb content are obtained. The frequency dispersion of the dielectric constant can also be noticed. However, the loci of the maxima at a given composition are only slightly influenced by the frequency (no relaxor behaviour). Furthermore, No difference between the values obtained on cooling and heating could be found (the curves shown in Fig. 6(a)–(c) were obtained on cooling). The peak values correspond to the ferroelectric to the paraelectric phase transition. The transition temperatures obtained at 1 kHz are: 325, 250 and 220°C for 0.05, 0.08 and 0.12 Nb respectively. It can also be seen that maximum dielectric constant values are obtained for the thin film containing 0.08 Nb, whereas the film containing 0.12 Nb is characterized by lowest values.

3.2.2. DC bias dependence of the dielectric constant (C-V-curves). The dependence of the small signal dielectric constant, ε', on DC bias field (C-V curves) is shown in Fig. 7.

All C-V curves show a "butterfly" appearance which is characteristic for the DC bias dependence of the polarization of ferroelectric materials. The dielectric constant shows a maximum at a voltage corresponding to the coercive field and decreases steeply with increasing

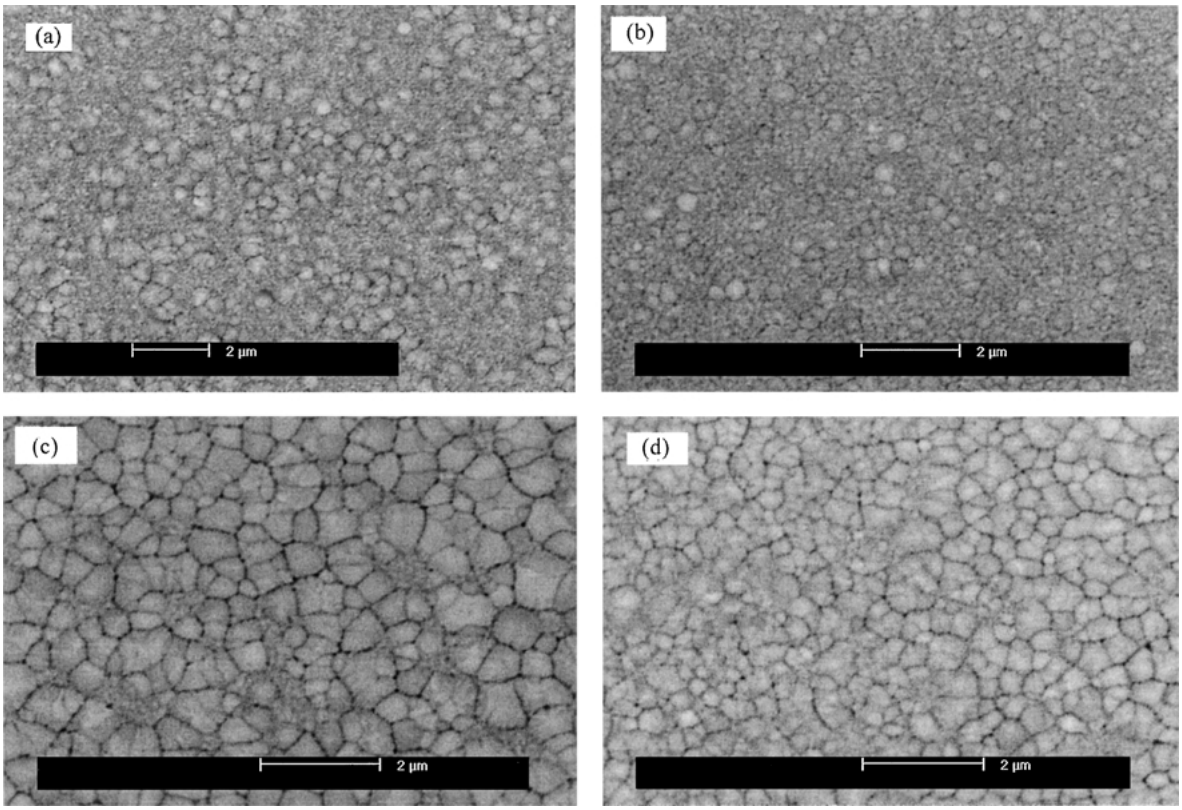

Fig. 5. BSE micrographs of the thin films processed with a seed layer and an PbO top layer before final annealing: (a) 0.0, (b) 0.05, 0.08 (c) and (d) 0.12 mol Nb.

DC bias. This behaviour is attributed to the contribution of domain wall oscillations to the dielectric constant [17, 18]. Similar observations can be made for the loss tangent. Figure 8 summarizes the peak values of ε' obtained at positive, $\varepsilon'_{+\max}$, and negative, $\varepsilon'_{-\max}$, bias fields as well as the values of ε'_0 obtained at the intersection of the butterfly curves which gives an approximate mean value of the small signal dielectric constant at 0 DC bias. The corresponding field values, E_c^+ and E_c^-, obtained from the C-V measurements are also shown. In comparison to the non-doped PZT film, the following observations can be made:

– The addition of Nb leads to a significant increase in the dielectric constant. Pure PZT is characterized by lowest dielectric constant which can be attributed to a high contribution of the disturbed interfacial layer (see below), the 111-texture of the film (Brooks et al. [14] report a higher dielectric constant for 100 textured PZT films) and the small grain size [10]. Particularly the small grain size is expected to affect domain wall contribution to permittivity through change in their density and mobility. The small grain size may also affect the stress state during the paraelectric to ferroelectric transition which in turns would affect the dielectric constant. The 0.08 Nb film is characterized by highest ε' values in the Nb containing films. This might be due to lower contribution from the disturbed interfacial layer, coarser grain size and the somewhat higher α_{100} (Table 1). These results do not agree with those reported by Klissurska et al. [11] who found decreasing ε' with increasing Nb content. This can be explained in terms of different microstructures and processing conditions.
– At room temperature the butterfly curves are asymmetric with respect to the values of the dielectric constant. This asymmetry is first pronounced for the PZT film at positive bias field, becomes weaker in the 0.05 Nb film and increases again for 0.08 and 0.12 Nb films (Fig. 8(a)).

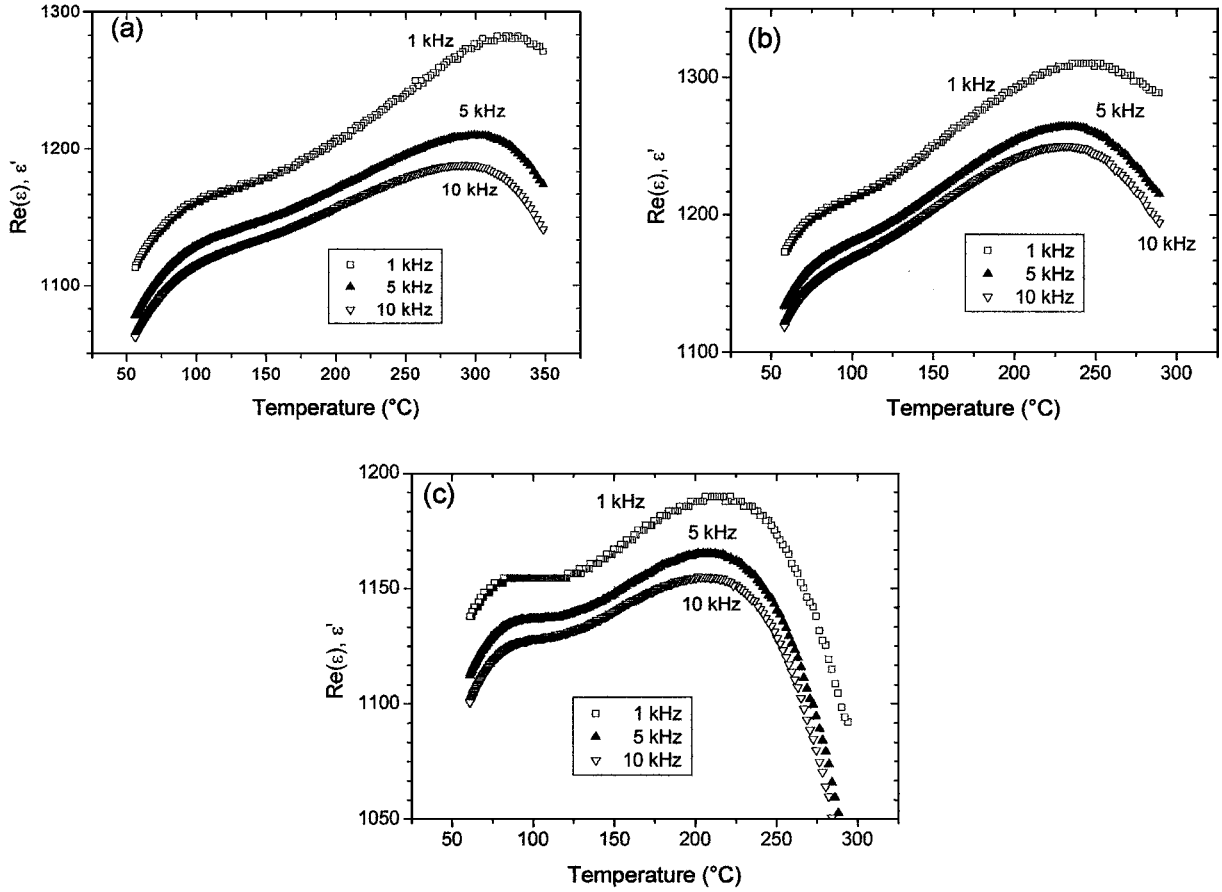

Fig. 6. Temperature dependence of the real part of the dielectric constant at different frequencies: 0.05 Nb (a), 0.08 Nb (b) and 0.12 Nb (c). The curves shown were obtained on cooling.

– At 100°C, the asymmetry almost disappears (for 0, 0.05 and 0.08 Nb) or becomes largely attenuated (for 0.12 Nb film).
– At room temperature, a strong negative built-in filed is found in pure PZT. The coercive field is shifted towards positive values. In case of Nb containing films, asymmetry towards positive values ($(E_c^+ - |E_c^-|)/2 > 0$) is also observed with 0.12 Nb film showing highest E_c^+ value. At 100°C a slight asymmetry is found to be towards negative values for PNZT films (positive built-in field), whereas a decrease of coercive fields is found for PZT. A strong negative built in field is, however, still present in PZT.
– Figure 9(a) shows the loss tangent, $\tan\delta$, at 1 kHz and 0 DC bias. It can be seen that $\tan\delta$ first increases for Nb contents up to 0.08 and then decreases strongly for 0.12 Nb. At 100°C, a similar behaviour is observed, though at much lower loss values.

The dependence of $\tan\delta$ on frequency illustrated in Fig. 9(b) shows a relaxation peak at frequencies which depend on the Nb content of the thin films, Fig. 9(b). The highest peak intensity is obtained for pure PZT whereas the Nb doped films show intensities more than one order of magnitude lower. Because all films have very similar thickness, the displacement of the maximum cannot be attributed to thickness effects [10]. Approximate values of f_m are 1 MHz for PZT and 0.05 Nb, 6 MHz for 0.08 and 4 MHz for 0.12 Nb containing PNZT films. Assuming that interfacial polarization is responsible for these peaks, the results would suggest that the addition of Nb leads to a decrease of the contribution of the interfacial layer to the dielectric behaviour of the thin films.

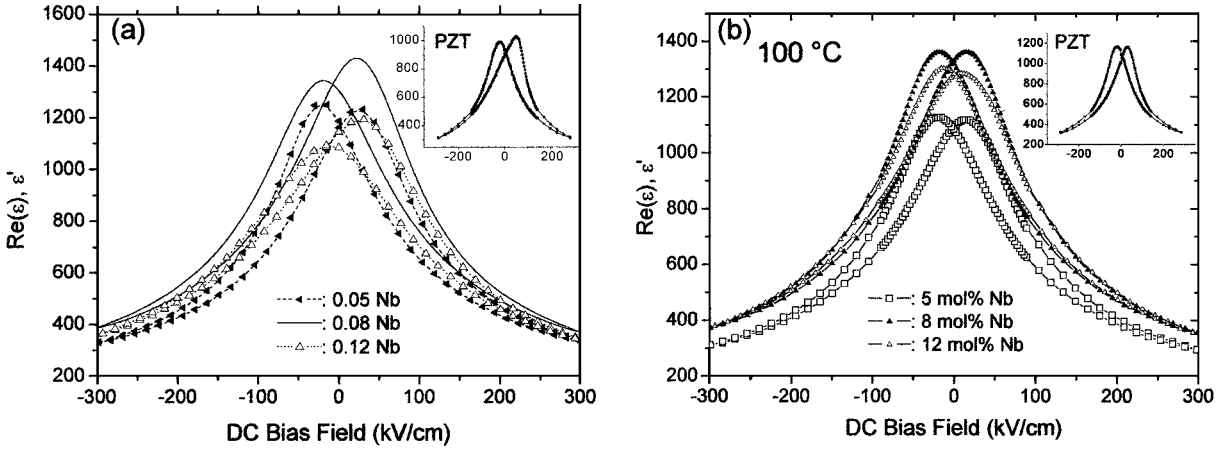

Fig. 7. Comparison of the C-V curves at 1 kHz of the thin films investigated: (a) at room temperature; (b) at 100°C. In both figures, the inset shows the corresponding C-V curve of pure PZT.

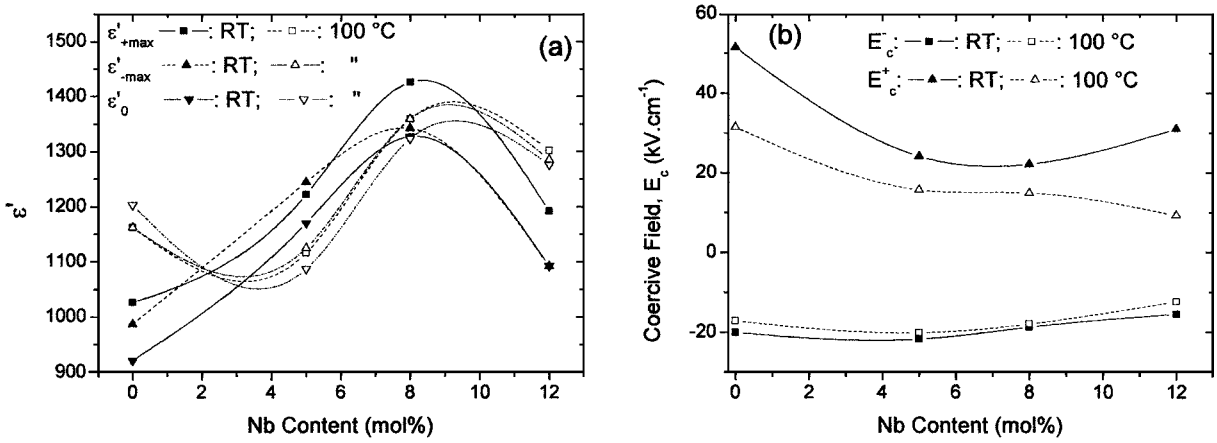

Fig. 8. (a) Variation of the dielectric constants, $\varepsilon'_{+\,\max}$ and $\varepsilon'_{-\,\max}$ at 1 kHz, corresponding to the maximums of the C-V curves with Nb content and temperature. The values of ε'_0 obtained at the points of intersections of the C-V curves are also shown. (b) Coercive field, E_c^- and E_c^+, corresponding to the maximums of ε'.

3.2.3. Ferroelectric hysteresis properties. Examples of the ferroelectric hysteresis loops are shown in Fig. 10 for non-doped PZT and PNZT films.

The ferroelectric properties depend on the Nb content. In comparison to PZT, slim hysteresis loops with lower coercive fields and remnant polarization values are obtained. The remnant polarization $+P_r$ decreases from 20 for PZT (0 mol Nb) to 12.0 for 0.05 Nb, 9.4 for 0.08 Nb and 7.5 μC·cm^{-2} for 0.12 Nb films. Furthermore, Saturation polarization is obtained at substantially higher drive fields than in PZT which points to domain pinning effects due to Nb additions. These results are consistent with those reported by Klissurska et al. [11, 12] who investigated the ferroelectric hysteresis properties of Nb doped PZT films with Nb in the range from 0 to 0.05 mol. The coercive field values were found to decrease from 59 kV/cm for pure PZT to 28 kV/cm for PNZT containing 0.12 Nb. These values are higher than those found from the C-V measurements, and can be attributed to the different methods of measurement involved (The C-V-method uses a slowly changing bias voltage and impedance capacity measurement whereas in the hysteresis measurement a pulse is applied to the contacts and the charge is integrated).

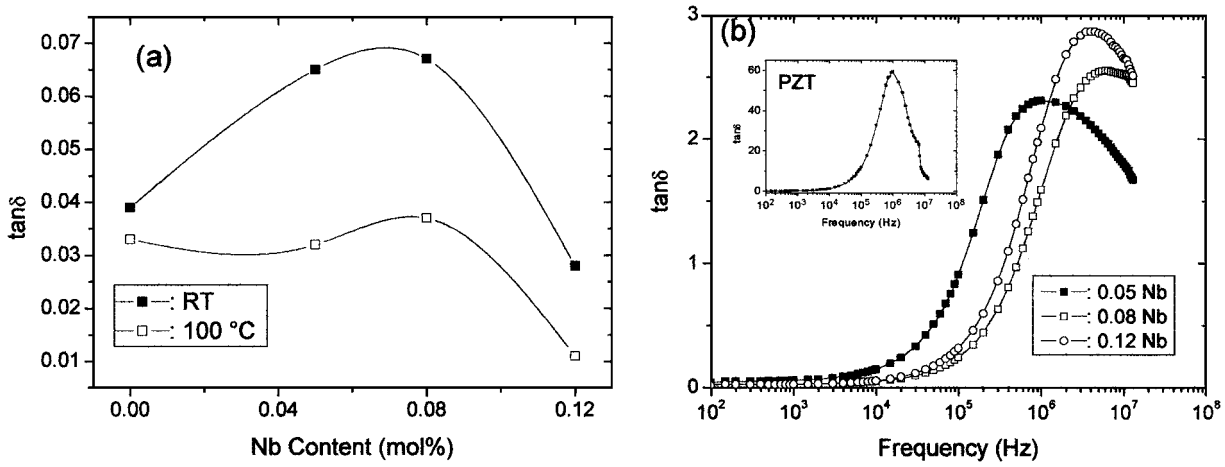

Fig. 9. Loss tangent, tan δ, (a) as function of Nb content, measured at 1 kHz and (b) as function of frequency showing loss peaks at different frequencies depending on the Nb content.

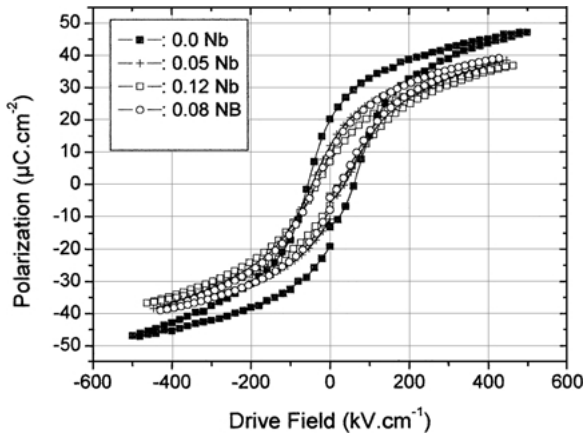

Fig. 10. Ferroelectric hysteresis loops of PZT and PNZT thin films containing 0.05 and 0.12 mol Nb.

4. Discussion

4.1. Microstructure

The results presented above show that it is possible to control the microstructure of Nb doped PZT thin films with compositions near the morphotropic phase boundary (MPB). The use of a seed layer and additional PbO coating are shown to be effective in minimising the amount of lead deficient pyrochlore which can be detrimental to the properties of the thin films. Furthermore a high degree of texture, grain size and grain shape control can be achieved. In previous work [14, 19], microsctructure of PZT thin films deposited on Pt bottom electrode has been shown to strongly depend on the pyrolysis schedule [14] and heating rate [14, 19]. This has been explained in terms of the formation of intermediate phases at the interface film/electrode [17]. A TiO_2 seed layer has been also reported to be effective in texture control [20]. Furthermore, the Zr to Ti ratio has been shown to control the amount of residual pyrochlore, grain size and grain shape [21]. Usually it is quite difficult to process pyrochlore free CSD PZT with Zr to Ti ratio in the vicinity of MPB or in the rhombohedral phase field [21], and the Nb doping has been shown to promote the formation of pyrochlore still more [11, 13]. A rosette like grain shape, as illustrated in Fig. 4, has been also shown to predominate in such films. It is thought that a better control of microstructure can be achieved via bringing the first layer to crystallization. The chemistry of the first layer is not yet clear, and should be investigated in more detail. However, SEM observations show a fine grained microstructure with well defined grain boundaries, and XPS analysis reveals PbO enriched surface and points to the formation of a reaction zone at the interface between ferroelectric and Pt electrode. It is expected that the microstructure of the seed layer which is controlled by all these factors will determine that of the following layers thus leading to a better control of microstructure. In contrast, the microstructure of non-seeded films will be influenced in a greater extent by such factors as surface nucleation sites and interfacial stresses which then lead to heterogeneous microstructures with non-controlled texture.

4.2. Electrical Properties

The effects of Nb content on the transition temperature, T_c, could be derived from the temperature dependence of the dielectric constant ε'. As expected, T_c decreases with increasing Nb content. This trend is well in agreement with the results reported elsewhere for PNZT ceramics with compositions in the tetragonal field of the PZ-PT phase diagram [22]. However, the values found in the present work are by far lower than those reported in [22], and can be explained by the higher Zr content of the present compositions. Furthermore, it has been shown [22] that Nb^{5+} preferentially substitutes the Zr sites which will shifts the composition towards the rhombohedral filed of the phase diagram with low T_c temperatures.

The C-V-curves can deliver, via their shape, valuable information about trapped charges and domain switching in ferroelectric thin films. At room temperature more or less pronounced vertical and horizontal asymmetries were observed for all thin films investigated. For pure PZT, ε' and E_c asymmetries are towards positive values (negative internal bias field). This suggests trapped positive charges, probably oxygen vacancies, at the disturbed interface layer between ferroelectric and bottom electrode. These charges are thought to affect domain switching reversal. The asymmetry is however much less pronounced for the 0.05 Nb containing film which can be explained in terms of effects of donor doping on reducing oxygen vacancies through:

$$Nb_2O_5 + V_O^{\bullet\bullet} \overset{(2TiO_2)}{\rightarrow} 2Nb_{Ti}^{\bullet} + 5O_O \qquad (2)$$

With increasing Nb doping concentration, the C-V curves show pronounced asymmetries towards positive ε' and E_c values, i.e $\varepsilon'_{+\max} > \varepsilon'_{-\max}$ and $E_c^+ > E_c^-$. This suggests that the distribution of space charge changes with increasing Nb content. Nb doping has been reported to lead to surface pyrochlore the fraction of which increases with increasing Nb content [11]. The existence of this low dielectric constant surface layer may lead to negative charge injection from the top electrode but this will rather result in a higher $\varepsilon'_{-\max}$. Furthermore, experimental evidence of the existence of this layer has not yet been brought, and its effects on polarization behaviour of PNZT have been questioned [12]. The fact that the loss tangent peaks are shifted towards higher frequencies with increasing Nb content also suggests that contributions from interfacial layers become weaker. The results may be qualitatively explained taking into account that Nb doping is balanced by A site (Pb) vacancies which compensate the p-type semi-conductivity of PZT. Increasing Nb content may lead to the formation of stable cation vacancy/hole dipoles at domain boundaries which may be responsible for the pinning of domains during DC bias reversal. The fact that the C-V curves become symmetrical at 100°C may support this mechanism in so far as dissociation of cation vacancy/hole dipoles is thermally activated. However, more investigations, particularly leakage current measurements as function of temperature, are needed in order to gain more insight in the nature of trapped charges in PNZT thin films.

Finally, the poor ferroelectric properties (lower remnant polarization, slant hysteresis loop) obtained for Nb doped films agree well with previous work [11, 12]. Effects of Nb in promoting pyrochlore formation [11] or increase of the area fraction of completely pinned domains with increasing Nb content have been advanced as possible mechanisms to explain these results [12]. However, there exists no experimental evidence of surface pyrochlore, and a plausible microstructural explanation of domain pinning effects is still lacking. Dausch and Haertling [10] investigated La doped PZT thin films and found slim hysteresis loops on Pt/Si substrates in comparison to films deposited on Ag foils and to bulk ceramics. They attributed this behaviour to difficulties in domain switching due to tensile stresses at the interface substrate/film, and to the existence of a reaction zone between PZT and Pt during processing. However, these explanations are not satisfactory, because if a reaction zone forms, it would also form in case of pure PZT and residual tensile stresses are also expected. Therefore, until detailed microstructural and electrical investigations have been done, at present, it can only be stated that Nb doping affects negatively domain switching in PZT thin films.

5. Conclusions

Nb doped PZT thin films (PNZT) with variable Nb content from 0 to 12 mol% have been prepared by spin-on sol-gel processing. A processing route involving seed layer and additional PbO coating has been developed to obtain homogeneous, fine grained microstructures with preferred 111/100 texture.

The temperature dependence of the dielectric constant shows that with increasing Nb content the

transition temperature decreases from 325 for 5% Nb to 220°C for 12% Nb. This is interpreted in terms of preferential occupancy of Zr sites by Nb which leads to a shift towards rhombohedral phase filed with lower transition temperatures. Nb is also shown to affect the C-V characteristics of PZT through modification of dielectric constant and coercive field asymmetries. With increasing Nb content, the asymmetries become pronounced. These asymmetries are very much attenuated as the testing temperature is increased. This is interpreted in terms of domain wall pinning by stable dipole configuration which can be dissociated upon thermal activation. Nb additions also lead to higher small signal dielectric constants in comparison to non- doped PZT, with maximum at 0.08 Nb. This is explained in terms of microstructural effects and lower contribution from the disturbed layer at the interface with the electrode. The loss tangents are lowered in Nb doped films, and a shift of the loss tangent peaks towards higher frequencies is found. This might be due to effects of Nb on the electrical properties of the interfacial layer. Finally, Nb is shown to be detrimental to ferroelectric properties in the range of concentration investigated.

Acknowledgment

The "Technologie-Stiftung Schleswig-Holstein" and the Federal Ministry of Education and Research (BMBF) are gratefully acknowledged for financial support of this work. The authors would like to thank Dr. V. Zaporojchenko, Technical Faculty, University of Kiel for conducting the XPS experiments, and Prof. F. Faupel for useful discussion.

References

1. D.L. Polla and L.F. Francis, *MRS Bulletin*, **21**(7), 59 (1996).
2. M. Okuyama, in *Sensors Update*, edited by H. Baltes, W. Göppel, and J. Heese (Wiley-VCH, Weinhein, Germany, 2000), p. 79.
3. K. Uchino, *Ferroelectric Devices* (Marcel Dekker, New York, 2000).
4. R.E. Jones and S.B. Desu, *MRS Bulletin*, **21**(6), 55 (1996).
5. S.B. Krupanidhi, in *Handbook of Thin Film Devices*, Vol. 5, edited by D.J. Taylor and M.H. Francombe (Academic Press, New York, 2000), p. 1.
6. B.A. Tuttle and R.W. Schwarz, *MRS Bulletin*, **21**(7), 49 (1996).
7. M. Es-Souni, M. Abed, A. Piorra, S. Malinowski, and V. Zaporojtchenko, *Thin Solid Films*, **389**, 99 (2001).
8. C. Voisard, K.G. Brooks, I.M. Reaney, L. Sagalowicz, A.L. Kholkin, N. Xanthopoulos, and N. Setter, *J. Eur. Cer. Sos.*, **17**, 1231 (1997).
9. R. Kurchania and S.J. Milne, *J. Mater. Sci.*, **33**, 659 (1998).
10. D.E. Dausch and G.H. Heartling, *J. Mater. Sci.*, **31**, 3409 (1996).
11. R.D. Klissurska, K.G. Brooks, I.M. Reaney, C. Pawlaczyk, M. Kosec, and N. Setter, *J. Am. Ceram. Soc.*, **78**, 1513 (1995).
12. R.D. Klissurska, A.K. Tagantsev, K.G. Brooks, and N. Setter, *J. Am. Ceram. Soc.*, **80**, 336 (1997).
13. M. Es-Souni, A. Piorra, C.-H. Solterbeck, and M. Abed, *Mater. Sci. Eng*. B, **86**, 237 (2001).
14. K.J. Brooks, R.D. Klissurska, P. Moeckli, and N. Setter, *J. Mater. Res.*, **12**, 531 (1997).
15. M. Es-Souni and A. Piorra, *Mater. Res. Bulletin*, **36**, 2563 (2001).
16. R. Dinu, M. Dinescu, J.D. Pedaring, R.A. Gunasekaran, D. Bäuerle, S. Bauer-Gogonea, and S. Bauer, *Appli. Phys.* A, **69**, 55 (1999).
17. S. Hiboux, P. Muralt, and T. Maeder, *J. Mater. Res.*, **14**, 4307 (1999).
18. C. Brennan, *Integr. Ferroelectrics*, **2**, 73 (1992).
19. S.-Y. Chen and I-Wei Chen, *J. Am. Ceram. Soc.*, **81**, 97 (1998).
20. G.J. Willems, D.J. Wouters, H.E. Maes, and R. Nouwen, *Integr. Ferroelectrics*, **15**, 19 (1997).
21. B.A. Tuttle, T.J. Headley, H.N. Al-Shareef, J.A. Voigt, M. Rodriguez, J. Michael, and W.L. Warren, *J. Mater. Res.*, **11**, 2309 (1996).
22. C.O. Paiva-Santos, C.F. Oliveira, W.C. Las, M.A. Zaghete, J.A. Varela, and M. Cilense, *Mater. Res. Bulletin*, **35**, 15 (2000).